46th AIAA Aerospace Sciences Meeting and Exhibit
7 - 10 January 2008, Reno, Nevada

AIAA 2008-842

On Application of Surface Measurement Techniques for Cryogenic High Reynolds Number Investigations on Wind Tunnel Models

Janin Leuckert*, Jan Domhardt*, Wolfgang Nitsche†

TU Berlin, Institute of Aeronautics and Astronautics, Berlin, 10587, Germany

Jürgen Quest‡

European Transonic Windtunnel GmbH, Cologne, 51147, Germany

High Reynolds number experiments make high demands on the wind tunnel model and on measurement techniques. A very smooth surface and a high spatial as well as temporal resolution are required. Especially for the detection of characteristic frequencies of flow instabilities, a high temporal resolution is needed. Since both the surface hot-wire and the newly developed Pressure Sensitive Copolymer technique provide these properties, these methods were applied to wind tunnel models for transition experiments carried out in the European Transonic Windtunnel and its pilot facility. The general measurement principles are described in detail to clarify their specific application to the various models. The performed experiments deal with the influence of leading edge roughness on the laminar turbulent transition. Additionally, investigations on the influence of the Reynolds number by changing total pressure and temperature has been carried out. The results are analysed using several methods.

Nomenclature

A	Area, mm^2
c	Chord length, mm
d_{33}	Piezoelectric constant of a normal charge displacement parallel to the pressure fluctuation, C/N
E	Electrical voltage, V
F	Frequency, Hz
L	Slat's total upper surface arc length, mm
M	Mach number
P	Pressure, Pa
p'	Pressure fluctuation, Pa
Q	Electrical charge displacement, C
Re	Reynolds number
R_z	Mean roughness of single roughness depth measured at 5 conjoined distances of same length, μm
s	Slat's local upper surface arc length, mm
T	Temperature, K
x	Local streamwise position, mm
α	Angle of attack, °
ϕ	Leading edge sweep angle, °
Subscript	
t	Total flow conditions
∞	Freestream flow conditions

*Research Scientist, Aerodynamics Section, Marchstr. 12-14 (Sek. F2)
†Professor, Aerodynamics Section, Marchstr. 12-14 (Sek. F2)
‡Chief Aerodynamicist & External Project Coordinator, Ernst-Mach-Strasse, AIAA senior member

I. Introduction

In recent years, several surface measurement techniques have been successfully applied for flow investigations on wind tunnel models. These measurement techniques can generally be divided into three categories. Some are developed to reach a high spatial resolution, e.g. Temperature Sensitive Paint (TSP).[1] Other sensors like Kulites are applied when a high temporal resolution is required. Surface hot-wire[2] as well as surface hot-film[3] arrays were developed to combine these advantages. Therefore, these methods are especially useful to detect unsteady flow phenomena, e.g. the laminar turbulent transition. Additionally, piezoelectric surface sensors also combine a high spatial and a high temporal resolution and thus have been used for transition detection[4,5] as well. As these sensors are based on a foil made of piezoelectric polymer polyvinylidene fluoride (PVDF), the application is limited to 2D curved surfaces. Hence, the Pressure Sensitive Copolymer (PSC)[6] coating, which is characterised by a high spatial as well as a temporal resolution, has been developed. PSC is based on the piezoelectrical properties of the copolymer of vinylidene fluoride and trifluoroethylene, whose dissolution can be sprayed on arbitrary surfaces. This newly developed measurement technique has already been applied for the characterisation of unsteady flow phenomena under ambient conditions.
High Reynolds number flow investigations entail very thin boundary layers on the wind tunnel models and thus a very smooth surface of the model is required. In addition, the characterisation of the boundary layer has to be performed by a flush mounted surface measurement technique in order to avoid sensor induced influences on the flow field. In the majority of cases concerning high Reynolds number experiments, the sensor techniques have to be operated either under pressurised or under cryogenic wind tunnel conditions. However, both methods are applied to increase the Reynolds number in the European Transonic Windtunnel (ETW) as well as in its pilot facility (PETW). Therefore, a highly resolutive flush mounted surface measurement technique operating under these conditions is required to perform transition experiments in these facilities. Very smooth surfaces can be produced by spraying the liquid Pressure Sensitive Copolymer onto the model's surface. Moreover, the optimisation of the electrical tapping and the signal path of PSC is primarily based on the results of the latest research of both the polyvinylidene fluoride foil as well as of the surface hot-wire technique and is thus suitable for highly integrated applications. Additionally, high spatial and temporal resolution can be achieved. The surface hot-wire technique has already been successfully established as a method for transition investigations under ambient flow conditions.[7,8] Just like the PSC, this measurement system can be flush mounted and provides a high resolution characterisation of the flow. Hence, both measurement techniques seem to be feasible for high Reynolds number transition experiments.

II. Surface Measurement Techniques

Especially at high Reynolds numbers, boundary layer investigations require a highly resolutive surface measurement technique, which additionally minimises sensor induced influences. The general set-up and principle of Pressure Sensitive Copolymer coating as well as the surface hot-wire measurement technique are described to show their capability to meet these requirements.

II.A. Pressure Sensitive Copolymer Coating

The Pressure Sensitive Copolymer measurement technique is based on the piezoelectric properties of the copolymer of vinylidene fluoride and trifluoroethylene. PSC surface coating reacts with an electrical polarisation to a mechanical force due to the piezoelectric effect. Thus, a local charge displacement (Q) is caused by an unsteady pressure (p') on a discrete sensing area ($A_{sensing}$). The charge displacement is also proportional to the piezoelectric constant of a normal charge displacement parallel to the pressure fluctuation (d_{33}), which depends on the piezoelectric material. The charge displacements of the sensing elements due to local pressure fluctuations are converted into measurable voltage (E) by electronic charge amplifiers which are connected to the electric tappings. The linear relationship between the local pressure fluctuation and the measurable output voltage is expressed in Eq. (1).

$$E(Q) = d_{33} \cdot p' \cdot A_{sensing} \tag{1}$$

The principle of Pressure Sensitive Copolymer coating is presented in Fig. 1. PSC is coated onto the sensing layer consisting of an electroconductive carrier material which is used for the electrical tapping. The discrete sensing areas and the electrical layout are produced by photo etching. Therefore, a high density of sensing areas can be realised and adapted to arbitrary applications. Additional surface roughnesses from the electrical connections are minimised by the separation of the sensing elements from the electrical taps. Consequently, PSC can be sprayed on a very thin multilayer circuit board or copper coated capton foil, depending on the application. The signal path can be shortened by the use of additional internal layers. A grounded layer can be included to reduce electrical noise, and a heating layer to improve the signal to noise ratio if necessary.

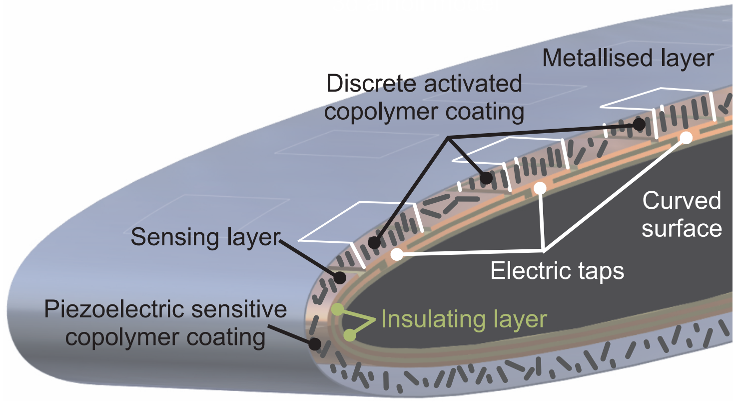

Figure 1. Principle of Pressure Sensitive Copolymer coating

The piezoelectric copolymer is sprayed onto the sensing layer. It is not yet sensitive because the crystallites of the copolymer are not orientated. Accordingly, the sensing elements of the PSC coating are discretely activated by a corona discharge, whereby a variable matrix of sensitive elements is achieved. Finally, the surface is vacuum metallised with a very thin layer of copper.

II.B. Surface Hot-wire Measurement Technique

The surface hot-wire measurement technique is based on the forced convection of a heated wire analogous to the conventional hot-wire anemometry. In Fig. 2 the principle of a single surface hot-wire is shown. In contrast to a conventional hot-wire, which is soldered on a probe, a surface hot-wire is welded over a narrow cavity on an electroconductive carrier material.[9] The cavity, which is produced by photo etching, is needed to reduce the heat flux into the substrate and thus increase the signal to noise ratio of the sensor compared with a surface hot-film. Due to the reduced heat flux into the material, the temporal resolution of a surface hot-wire is increased by a factor of ≈ 1.5. Additional cavities next to the wire contacts are used for the power supply. Furthermore, the chemical etching process of manufacturing a surface hot-wire sensor enables the realisation of tightly packed sensor layouts depending on the application.

After the etching process, all cavities are filled with surfacer to reduce local roughness effects. A platinum-coated tungsten wire with a diameter of $\o = 5\ \mu$m is used as the sensor. Depending on the application of an array, the carrier material can be a copper coated capton foil or a glass fibre circuit board, which is less flexible but more rugged.

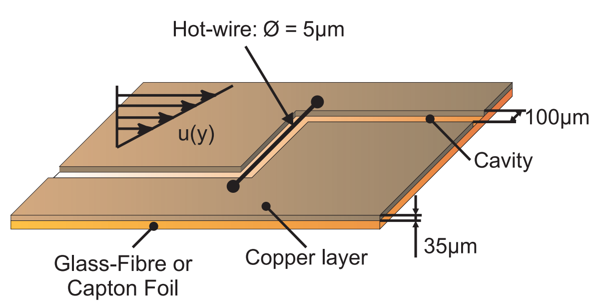

Figure 2. Principle of a single surface hot-wire sensor

The surface hot-wire sensors are operated in the constant temperature mode by using Wheatstone bridges. The surface hot-wires are sensitive to the flow velocity just like conventional hot-wires. However, the near-wall configuration of the surface hot-wires allows a correlation between the flow velocity (u) and the local wall shear stress using the viscous sublayer law, because of the small wire diameter and the constant distance to the wall (y). Therefore, the Wheatstone bridge output voltage can be calibrated against the local wall shear stress. However, qualitative boundary layer analysis can already be performed due to the proportionality between the output voltage level and the local wall shear stress amplitudes.

III. Application of Surface Sensors for High Reynolds Number Transition Experiments

Several test campaigns involving cryogenic high Reynolds number transition experiments were performed in the European Transonic Windtunnel and in its pilot facility within the framework of diverse EC Projects. A 14-bit multi-channel data acquisition system was used for all test campaigns. In order to characterise the transition, the signals were analysed using different statistical quantities. The Root Mean Square (RMS) values were calculated to obtain information about the mean fluctuation amplitude. Increased RMS values indicate regions with high levels of local fluctuations, e.g. a transitional boundary layer.[10] Furthermore, the transition can be characterised by analysing the skewness of the fluctuating signals.[11] A laminar boundary layer is characterised by a skewness of about zero. When the laminar boundary layer starts to become transitional, the skewness reaches a maximum followed by a crossing zero in the transition area. After reaching a minimum (late stage of transition), the skewness rises again towards zero for a turbulent boundary layer. Additionally, the power spectra were considered to determine the characteristic frequency range of the boundary layer instabilities.

III.A. Transition Detection on a 2D Airfoil Model by Applying Pressure Sensitive Copolymer Coating

The influence of leading edge roughness on the laminar turbulent transition was investigated within the framework of the EC Project „Fliret". The experiments have been carried out for a 2D curved airfoil model with a chord length of $c = 100\ mm$ in the Pilot European Transonic Windtunnel. This model was instrumented with Pressure Sensitive Copolymer coating. Additionally, the model was also equipped with Temperature Sensitive Paint (TSP) by the DLR (German Aerospace Center). Moreover, both the suction and the pressure side of the model were equipped with pressure taps to measure the mean pressure distribution.

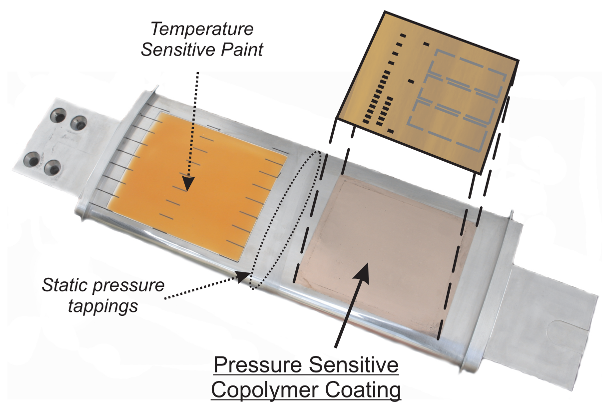

Figure 3. Instrumented 2D airfoil model for transition experiments on the influence of leading edge roughness performed in the PETW

III.A.1. Experimental Set-up

The Pressure Sensitive Copolymer was coated onto a special multilayer circuit board. For its flush mounted application, a cavity of $70mm$ (streamwise) $\times$ $82mm$ (spanwise) was machined into the surface of the model. The instrumented PETW model is presented in Fig. 3. The PSC sensing layer consisted of 24 active elements covering a range of $0.20 \leq x/c \leq 0.74$. These sensing elements were staggered in three streamwise rows. Each element had a size of $1.5\ mm$ (streamwise) $\times$ $3\ mm$ (spanwise). The first row consisted of 15 sensing elements with the highest density in the area of $0.20 \leq x/c \leq 0.50$. Due to the expected 2D character of the flow, a second row consisting of six active elements was shifted $1.5\ mm$ streamwise and $7\ mm$ spanwise to increase the spatial resolution in the range of $0.21 \leq x/c \leq 0.365$. The additional three active elements of the third row were placed as reference elements for the first row at $x/c = 0.20$, 0.50 and 0.74.

The PSC signal path was shortened by designing the final layer with integrated electronic charge amplifiers. The necessary electronic components were soldered directly onto the final layer of the PSC circuit board. Three deeper cavities were machined additionally into the PSC pocket for the charge amplifiers. The PSC coated circuit board with its electronic components was flush mounted into the model by a vacuum gluing method to minimise additional surface roughness and to prevent curvature modifications. Finally, the Pressure Sensitive Copolymer coating was vacuum metallised with a very thin copper layer (200 nm).

All experiments were performed at a constant freestream Mach number of $M_\infty = 0.24$ with different angles of attack and Reynolds numbers in the range of $1.0 \times 10^6 \leq Re \leq 4.0 \times 10^6$. In a first step, the base flow was characterised for the reference leading edge roughness of $R_z = 1\ \mu m$. Afterwards, the leading edge was roughened stepwise in the area between 5% chord of the pressure side and 2% chord of the suction side.

III.A.2. Experimental Results

The RMS distributions at $Re = 1.0 \times 10^6$ ($P_t = 186\ kPa$, $T_t = 290\ K$) and various angles of attack for the reference roughness of $R_z = 1\mu m$ are shown in Fig. 4 (a). The laminar flow over the sensing area is represented by the constant low RMS level at $\alpha_\infty = 2.14°$. The transitional boundary layer along with increased pressure fluctuations is detected by the step-up of the RMS values at $x/c > 0.56$, when the angle of attack is increased to $\alpha_\infty = 2.64°$. Due to the adverse pressure gradient caused by the further increase of the angle of attack, the rise of the RMS values is shifted upstream, thus indicating the upstream shift of the laminar turbulent transition. The turbulent boundary layer downstream of $x/c \geq 0.41$ for $\alpha_\infty = 3.64°$ and $x/c \geq 0.38$ for $\alpha_\infty = 4.14°$ is detected by the nearly constant but significantly higher RMS level compared with the laminar flow.
The influence of increasing Reynolds number on transition at $\alpha_\infty = 1.14°$ is presented in Fig. 4 (b). The boundary layer is laminar all over the sensing area for Reynolds numbers $Re = 1.0 \times 10^6$ ($P_t = 186\ kPa$, $T_t = 290\ K$) and $Re = 1.5 \times 10^6$ ($P_t = 278\ kPa$, $T_t = 290\ K$) detected by the constant low RMS level. When increasing the Reynolds number to $Re = 2.0 \times 10^6$ ($P_t = 211\ kPa$, $T_t = 190\ K$), the boundary layer becomes transitional between $0.38 < x/c < 0.62$, indicated by the rise of the RMS values.

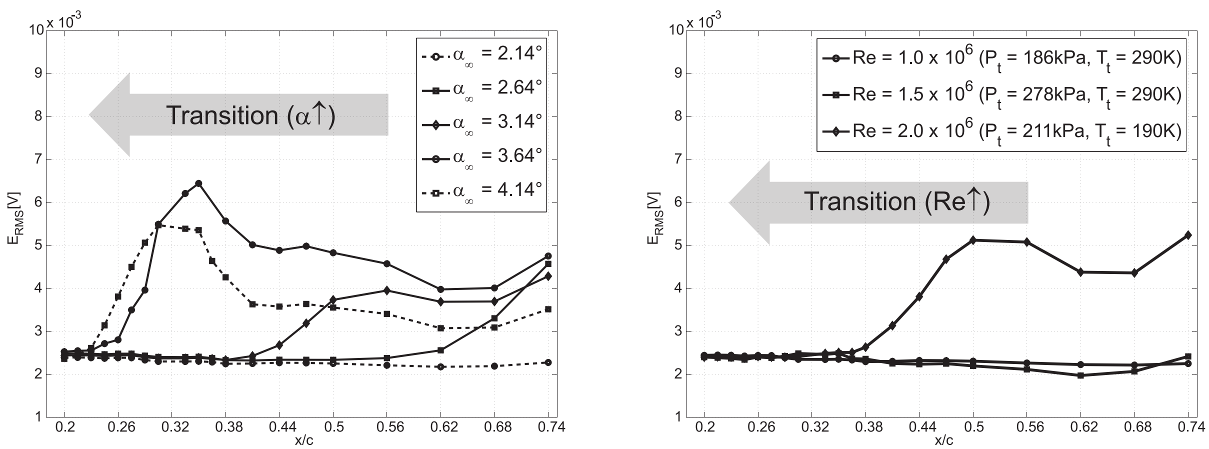

(a) Various angles of attack and $Re = 1.0 \times 10^6$ ($P_t = 186\ kPa$, $T_t = 290\ K$)

(b) Various Reynolds numbers and $\alpha_\infty = 1.14°$

Figure 4. RMS distributions of PSC obtained at reference leading edge roughness of $R_z = 1\ \mu m$ and $M_\infty = 0.24$

Once more, the influence of the adverse pressure gradient on transition is shown in Fig. 5 (a). Here the RMS distributions obtained at $Re = 2.0 \times 10^6$ ($P_t = 370\ kPa$, $T_t = 290\ K$) and various angles of attack for the leading edge roughness of $R_z = 7\ \mu m$ are presented. Again the upstream shift of transition due to the increased angle of attack is noticeable.
The dependence of transition on the Reynolds number at a fixed angle of attack ($\alpha_\infty = 1.00°$) and $R_z = 7\ \mu m$ is shown in Fig. 5 (b). The boundary layer is laminar all over the sensing area at $Re = 1.0 \times 10^6$ ($P_t = 186\ kPa$, $T_t = 290\ K$), whereas it becomes transitional at the end of the sensing area at $Re = 1.5 \times 10^6$ ($P_t = 179\ kPa$, $T_t = 290\ K$). A further increase of the Reynolds number leads to slight upstream shift of transition.
The influence of various leading edge roughness on the laminar turbulent transition at Reynolds number $Re = 1.0 \times 10^6$ ($P_t = 186\ kPa$, $T_t = 290\ K$) and different angles of attack is shown in Fig. 6. The constant low RMS level for $\alpha_\infty = 1.00°$ characterises the laminar boundary layer all over the sensing area, which is independent of increasing leading edge roughness. When the angle of attack is increased to $\alpha_\infty = 4.00°$, the transition is indicated by the rising RMS amplitudes but there is no significant shift of the transition area.

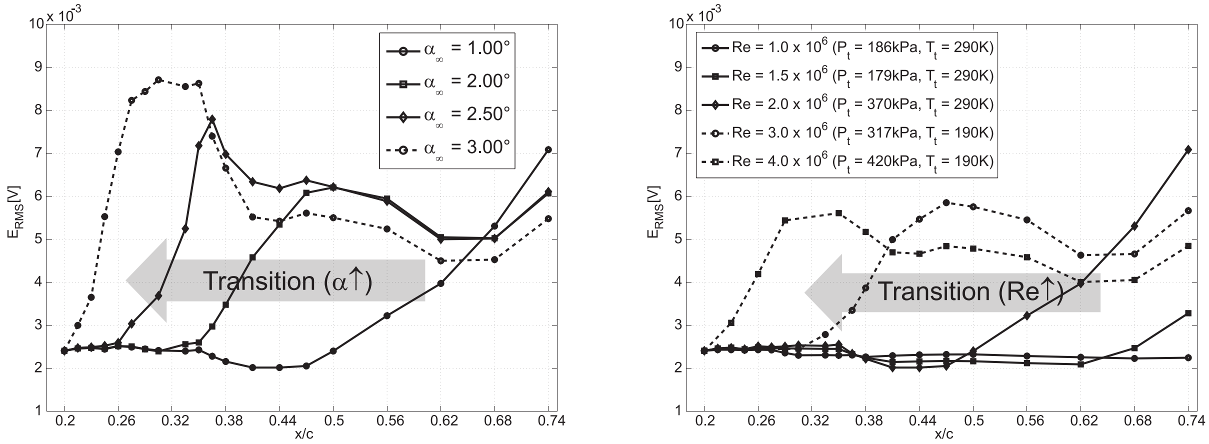

(a) Various angles of attack and $Re = 2.0 \times 10^6$ ($P_t = 370\ kPa$, $T_t = 290\ K$)

(b) Various Reynolds numbers and $\alpha_\infty = 1.00°$

Figure 5. RMS distributions of PSC obtained at leading edge roughness of $R_z = 7\ \mu m$ and $M_\infty = 0.24$

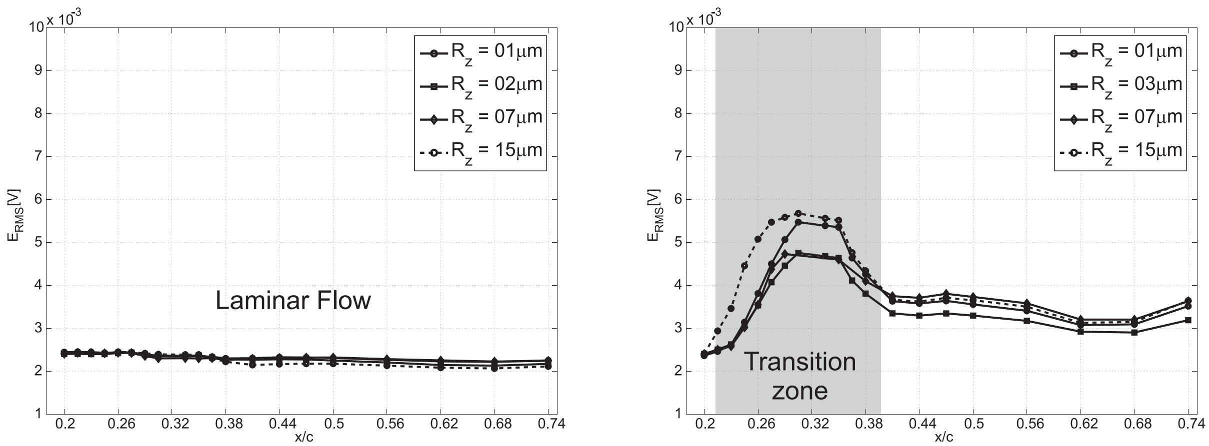

(a) $\alpha_\infty = 1.00°$

(b) $\alpha_\infty = 4.00°$

Figure 6. RMS distributions of PSC obtained at various leading edge roughness at $Re = 1.0 \times 10^6$ ($P_t = 186\ kPa$, $T_t = 290\ K$) and $M_\infty = 0.24$

III.B. Transition Detection by Applying Surface Hot-wire Arrays

Within the framework of the EC Project ,,Eurolift II", the performance of the surface hot-wire measurement technique was investigated under cryogenic conditions. In preparation for the transition experiments performed in the European Transonic Windtunnel on a slat of a 3D swept high-lift configuration, preliminary experiments on a 2D swept airfoil model were performed in the pilot facility. In addition to the surface hot-wire array, both models were equipped with a surface hot-film array by the DLR. All experiments were performed at a constant freestream Mach number of $M_\infty = 0.2$.

III.B.1. Experimental Set-up of a 2D Swept Airfoil Model Investigated in the PETW

The transition experiments performed in the PETW were carried out for a 2D airfoil model with a chord length of $c = 68mm$ and a leading edge sweep angle of $\phi = 25°$, shown in Fig. 7. The applied surface hot-wire array was based on an especially designed layout consisting of streamwise as well as spanwise oriented sensors covering an area of $0.10 \leq x/c \leq 0.21$. The surface hot-wire array was based on a copper coated capton foil applied from the suction side around the leading edge to the pressure side. To minimise additional roughness, the surface hot-wire array was applied to a cavity machined into the surface of the model utilising a vacuum gluing method. By using this flexible capton foil, the sensors were connected on the pressure side to very thin insulated cooper wires with a diameter of $\o = 0.2\ mm$, which were laid into a cut inside the wing to minimise the influence on the flow field.

The insulated wires were connected to co-axial cables for the data link to the multi-channel constant temperature anemometer outside the test section. In preparation for the ETW experiments, special micro-coax cables were used with a length of $l = 25m$ and very low specific cable resistance. Their resistances were significantly lower than the sensor resistances. Furthermore, two-thirds of the cable length were laid into the plenum of the wind tunnel to simulate the test conditions of the main experiments in the ETW at low temperatures.

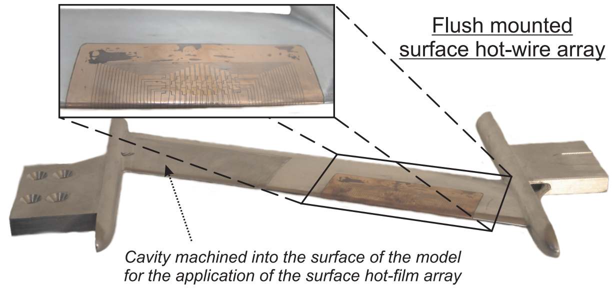

Figure 7. Surface hot-wire array on a 2D swept airfoil model for transition experiments performed in the PETW

III.B.2. Experimental Results obtained on the 2D Swept Airfoil Model

The experiments on the influence of the adverse pressure gradient on the laminar turbulent transition have been carried out for a Reynolds number of $Re = 0.42 \times 10^6$ at ambient flow conditions ($P_t = 120\ kPa$, $T_t = 290\ K$). The RMS distributions of the streamwise surface hot-wire sensors at various angles of attack are presented in Fig. 8 (a). The laminar flow is indicated by the very low RMS values at $\alpha_\infty = 4.0°$ all over the sensor area of $0.10 \leq x/c \leq 0.21$. An increase of the angle of attack to $\alpha_\infty = 5.0°$ leads to a significant rise of the RMS values downstream of $x/c > 0.10$, thus characterising the laminar turbulent transition. Furthermore, the rise of the RMS values is smaller than for $\alpha_\infty = 6.0°$, where a very high RMS level is noticeable with a maximum at $x/c = 0.135$. Additionally, a drop of the RMS values is noticeable for this increased angle of attack indicating the turbulent flow downstream of $x/c \geq 0.17$ at $\alpha_\infty = 6.0°$. Therefore, the transition is shifted upstream due to the adverse pressure gradient.

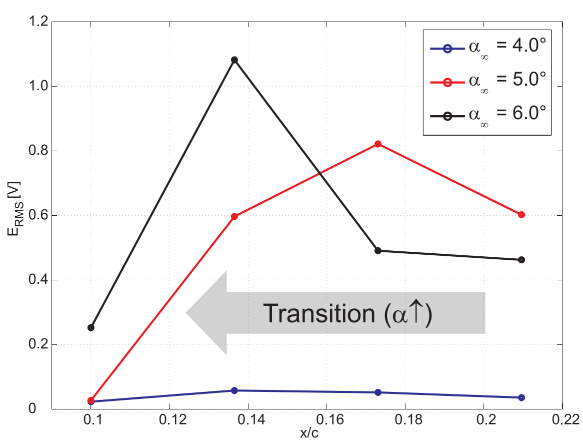

(a) RMS distributions of the streamwise sensors

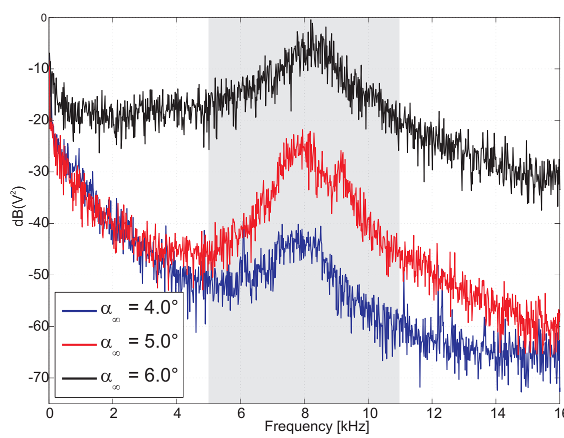

(b) Power spectra obtained at the streamwise position $x/c = 0.10$

Figure 8. Surface hot-wire signals at various angles of attack, $Re = 0.42 \times 10^6$ **(**$P_t = 120\ kPa$, $T_t = 290\ K$**) and** $M_\infty = 0.2$

The power spectra for the flow conditions at a streamwise position of $x/c = 0.10$ are shown in Fig. 8 (b). Although no significant rise of the RMS values was detected for $\alpha_\infty = 4.0°$, the dominant frequency range caused by the Tollmien-Schlichting (TS) instability waves is already visible and can be determined to $5.0 \leq F \leq 11\ kHz$. When increasing the angle of attack to $\alpha_\infty = 5.0°$, the characteristic frequency range is clearly amplified compared to $\alpha_\infty = 4.0°$. A further increase of the angle of attack leads to a general rise of the frequency level but the spectrum is still dominated by the characteristic frequency range. Therefore, the late stage of transition is indicated at this streamwise position and $\alpha_\infty = 6.0°$, corresponding to the RMS values.

In order to clarify the results, the time traces of the surface hot-wire sensors at $\alpha_\infty = 5.0°$ are presented in Fig. 9. In accordance to the RMS distribution, very low fluctuating amplitudes were obtained at $x/c = 0.10$. A detail of this time trace shows the typical TS-wave packages, whose centre frequency of $F = 8.0\ kHz$ was also indicated in the power spectra. A significant rise of the signal amplitudes is noticeable further downstream. However, the downstream amplification of the wave packages can not be definitely determined and thus characterises the late stage of transition.

The dependence of the characteristic frequency range on increasing Reynolds number is shown in Fig. 10. The spectra for a selected surface hot-wire sensor at the streamwise position of $x/c = 0.10$ and $\alpha_\infty = 3.0°$ demonstrate the step-up of the centre frequency with increasing Reynolds number. The centre frequency of $F = 8.4\ kHz$ at $Re = 0.42 \times 10^6$ $(P_t = 120\ kPa,\ T_t = 290\ K)$ is slightly higher as already determined due to the lower angle of attack. In addition, it is obviously shifted to $F = 11.2\ kHz$ as the Reynolds number is increased to $Re = 1.11 \times 10^6$. In order to evaluate a possible influence of total pressure and temperature, two curves representing the same Reynolds number ($Re = 1.11 \times 10^6$) at different total temperature and pressure are shown in comparison. The general magnitude level differs slightly due to the individual adjustment of the surface hot-wire sensors for each flow temperature. Additionally, there is an increase of the magnitude at $F = 7.5\ kHz$ for the low temperature, which is probably caused by the electronics due to the insufficient adjustment of the sensor. However, the characteristic frequency range can be concordantly determined for both flow conditions. Moreover, the magnitude level is significantly increased all over the frequency range and thus indicates the later stage of the transition compared to $Re = 0.42 \times 10^6$ for the same angle of attack. An additional rise in the Reynolds number leads to a further shift of the centre frequency to $F = 12.6\ kHz$ for $Re = 3.15 \times 10^6$ $(P_t = 290\ kPa,\ T_t = 125\ K)$ and $F = 13.8\ kHz$ for $Re = 4.25 \times 10^6$ $(P_t = 387\ kPa,\ T_t = 125\ K)$.

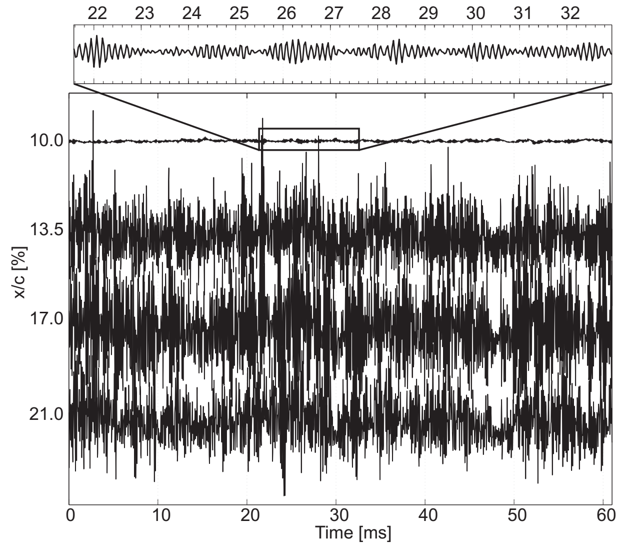

Figure 9. Time traces of the streamwise surface hot-wire sensors measured at $\alpha_\infty = 5.0°$, $Re = 0.42 \cdot 10^6$ $(P_t = 120\ kPa,\ T_t = 290\ K)$ and $M_\infty = 0.2$

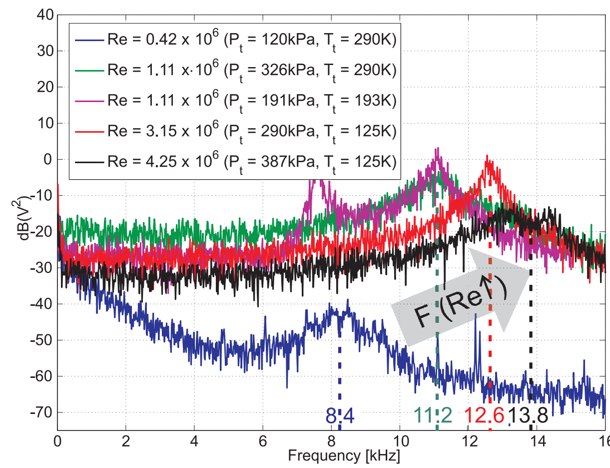

Figure 10. Power spectra of a selected surface hot-wire sensor $(x/c = 0.10)$ at various Reynolds numbers, $\alpha_\infty = 3.0°$ and $M_\infty = 0.2$

III.B.3. Experimental Set-up of a 3D Slat of an Industrial High-lift Configuration Investigated in the ETW

Additional transition measurements using surface hot-wire sensors have also been performed in the European Transonic Windtunnel. These experiments were carried out for a half model of a 3D industrial high-lift configuration, where the surface hot-wire array was applied at the leading edge inboard slat. The 3D slat equipped with the surface hot-wire array is shown in Fig. 11. The sensor array was especially designed and based on a copper coated capton foil due to the strong curvature of the slat. This sensor array consisted of 2 streamwise rows with a distance of 2.25 mm and a spanwise spacing of 6 mm. The first row with 20 sensors covered a downstream area of $0.27 \leq s/L \leq 0.89$, whereas a spatial resolution of $0.32 \leq s/L \leq 0.66$ was reached with the second row consisting of 11 sensors.

As in the preliminary experiments in the PETW, the sensors were connected to very thin insulated wires to minimise the influence on the flow field. These insulated wires were laid on the pressure side of the slat and were connected to the special micro-coax cables situated in the fuseloge. The data link to the multi-channel constant temperature anemometer was obtained in the fuselage. In addition to the $31st$ surface hot-wire sensors, the $32nd$ sensor was shorted in order to determine the decreasing cable resistance under cryogenic flow conditions. Therefore, the sensor resistances were defined more precisely and the adjustment of the surface hot-wire sensors was improved at these flow conditions.

III.B.4. Experimental Results obtained on the 3D Slat

The RMS distributions of the first surface hot-wire row obtained at $Re = 2.36 \times 10^6$ ($P_t = 150\ kPa$, $T = 288\ K$) and various angles of attack are presented in Fig. 12 (a). The laminar flow is present for the angle of attack of $\alpha_\infty = 6.0°$, as is clearly indicated by the low RMS level. Increasing the angle of attack to $\alpha_\infty = 8.0°$ forces the transition zone into the sensor region close to the trailing edge, which is indicated by a rapid growth of the amplitudes of the RMS values in the area of $0.56 < s/L \leq 0.73$. Additionally, the enlarged detail of the time traces obtained at $s/L = 0.60$ (Fig. 12 (c)) clearly represents the TS waves packages and thus indicates the TS dominated transition. Downstream of $s/L > 0.83$ the RMS values decrease at a raised level compared to the laminar flow, characterising the turbulent state. An increase of the angle of attack causes a rise of the adverse pressure gradient and forces a significant upstream shift of the transition into the area of $0.45 < s/L < 0.70$ at $\alpha_\infty = 10.0°$. Furthermore, the transition is shifted slightly upstream when further increasing the angle of attack to $\alpha_\infty = 12.0°$.

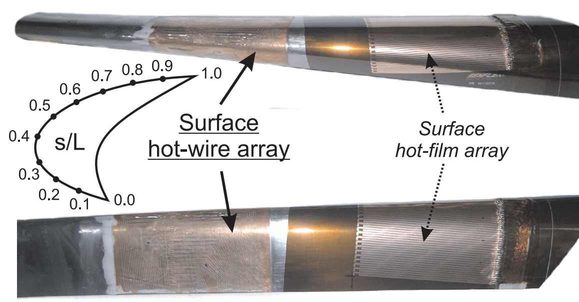

Figure 11. Instrumented 3D slat for transition experiments performed in the ETW

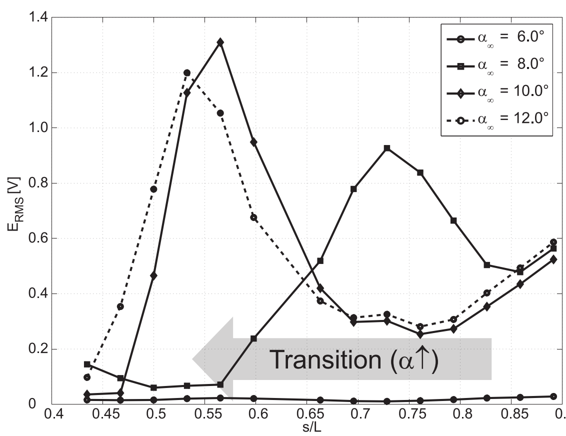

(a) RMS distributions at various angles of attack

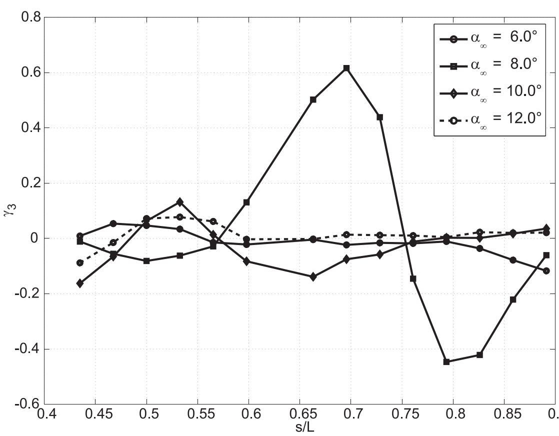

(b) Skewness at various angles of attack

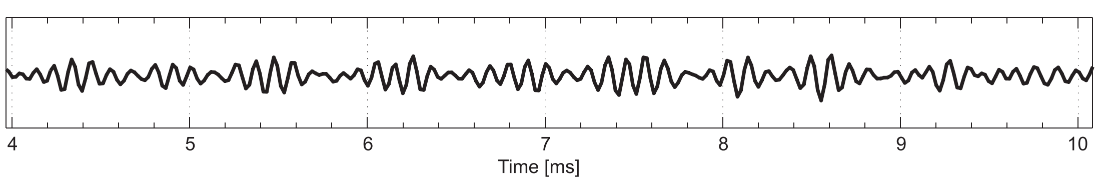

(c) Enlarged detail of the time trace measured at $s/L = 0.60$ and $\alpha_\infty = 8.0°$

Figure 12. Signals of the surface hot-wire sensors at $Re = 2.36 \times 10^6$ ($P_t = 150\ kPa$, $T_t = 288\ K$) and $M_\infty = 0.2$

In correspondence to the RMS values, the skewness also indicates the boundary layer stage as shown in Fig. 12 (b). The skewness of about zero describes the laminar boundary layer all over the sensor area at $\alpha_\infty = 6.0°$ as well as the area up to $s/L \leq 0.55$ at $\alpha_\infty = 8.0°$. Downstream of that area, the boundary layer becomes transitional, which is characterised by the rise of the skewness towards a maximum followed by a crossing zero at $s/L = 0.75$. After reaching a minimum, the skewness rises slightly towards zero downstream of $s/L > 0.83$ which is typical for the turbulent state. The distribution of the skewness described is not found for the increased angles of attack. However, there is a slight rise of the skewness in the upstream area of the slat at $s/L < 0.60$ for $\alpha_\infty = 10.0°$ and $\alpha_\infty = 12.0°$. Therefore, the sensor density in this area is insufficient for a detection of the maximum and minimum of the skewness which would be necessary for the definite characterisation of the boundary layer.

The influence of Reynolds number on the laminar turbulent transition is presented for $\alpha_\infty = 0.0°$ in Fig. 13 (a). For the Reynolds number of $Re = 5.38 \times 10^6$ ($P_t = 340\ kPa$, $T_t = 289\ K$) very low RMS values are detected compared to the RMS distribution obtained at $\alpha_\infty = 6.0°$ and $Re = 2.36 \times 10^6$ (Fig. 12 (a)). Furthermore, there is a slight rise of the RMS level at $s/L > 0.83$. Therefore, the transition occurs very close to the trailing edge for these flow conditions. As the Reynolds number is increased to $Re = 9.00 \times 10^6$ ($P_t = 348\ kPa$, $T_t = 200\ K$), high RMS values are detected close to the leading edge of the slat, which decrease further downstream to a constant high level. The time traces of the surface hot-wire sensors obtained for same flow conditions are presented in Fig. 13 (b). Very strong fluctuating amplitudes are obtained in the area of $0.43 \le s/L \le 0.50$. Additionally, no characteristic wave package is visible. Moreover, the amplitudes drop, followed by highly fluctuating signals downstream. Considering the leading edge radius as well as the sweep angle of the slat, these high fluctuations are probably caused by attachment line transition. For Reynolds number $Re = 15.20 \times 10^6$ ($P_t = 355\ kPa$, $T_t = 138\ K$) the RMS distribution is also significantly increased compared to the lowest Reynolds number. Furthermore, no characteristic structures were detected within the time traces of the sensor signals, indicating the turbulent boundary layer all over the sensor area.

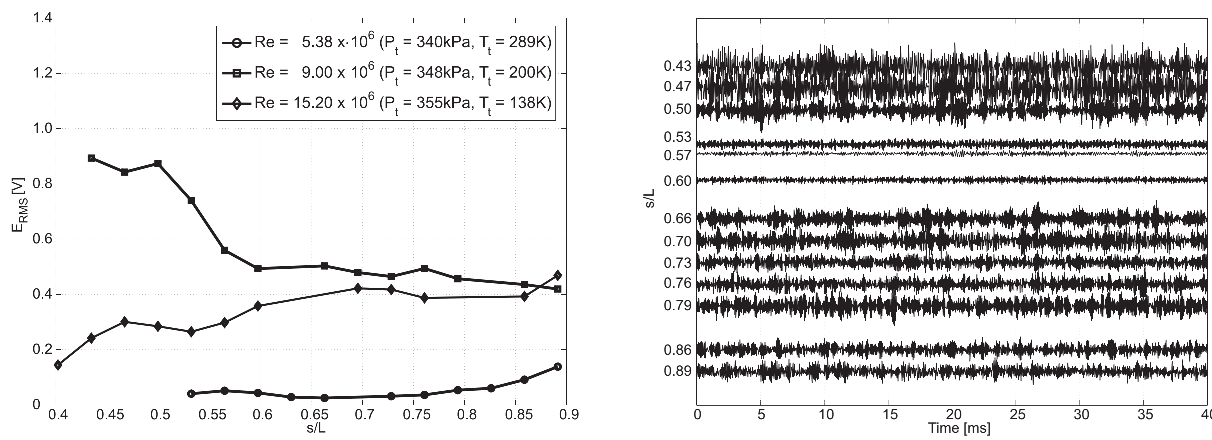

(a) RMS distributions at various Reynolds numbers

(b) Time traces at $Re = 9.00 \times 10^6$ ($P_t = 348\ kPa$, $T_t = 200\ K$)

Figure 13. Signals of the streamwise surface hot-wire sensors at $\alpha_\infty = 0.0°$ and $M_\infty = 0.2$

IV. Conclusion

The newly developed Pressure Sensitive Copolymer coating and the surface hot-wire array technique were successfully applied to wind tunnel models investigated in the European Transonic Windtunnel as well as in its pilot facility. Transition experiments were carried out at low freestream Mach numbers in the range of $0.20 \le M_\infty \le 0.24$ and various flow conditions.

The aim was to investigate the influence of the leading edge roughness on a 2D airfoil model equipped with PSC in the PETW. Therefore, the leading edge roughness was varied over the range $1\ \mu m \le R_z \le 15\ \mu m$. The results did not show a significant influence of the roughness at Reynolds number $Re = 1 \times 10^6$. However, there was an upstream shift of the transition area due to the adverse pressure gradient enforced by an increase of the angle of attack. Additionally, the upstream shift of the transition as a result of increased Reynolds number was demonstrated.

Furthermore, two models were equipped with surface hot-wire arrays for experiments on transition detection performed in the PETW as well as in the ETW. The dependence of transition on the angle of attack and Reynolds number was shown using this technique. Moreover, the characteristic Tollmien-Schlichting wave packages as well as the increase of the frequency range due to a rise of the Reynolds number were detected. The results obtained for both surface measurement techniques clearly demonstrate their capability for transition experiments on wind tunnel models at high Reynolds numbers and under cryogenic conditions.

Acknowledgments

The research on the Pressure Sensitive Copolymer coating technique is supported within the framework of the EC Projects ,,Flight Reynolds Number Testing (Fliret)" and ,,Testing for Laminar Flow on New Aircraft (Telfona)" as well as within the DFG priority programme ,,Image based measuring techniques for the flow analysis". In addition, the experiments concerning the cryogenic application of the surface hot-wire technique were supported within the framework of the EC Project ,,European High Lift Programme (Eurolift) II". The authors especially thanks the ETW crew as well as the DLR partners for their close collaboration.

References

[1]Fey, U., Egami, Y., Klein, C., *Using cryoTSP as a tool for transition detection and instability examination at high Reynolds numbers*, New Results in Numerical and Experimental Fluid Mechanics VI, Notes on Numerical Fluid Mechanics and Multidisciplinary Design Vol. 96, pp. 227-237, Springer, Germany, 2007.

[2]Spazzini, P.G., Iuso, G., Onorato, M., Zurlo, N., *Design, Test and Validation of a Probe for Time-Resolved Measurement of Skin Friction*, Measurement Science and Technology Vol. 10, pages 631-639, 1999

[3]Sheplak, M., Spina, E.F., McGinley, C.B., *Progress in Hot-Film Anemometry for Hypersonic Flow*, Experimental Thermal and Fluid Science Vol. 13, pages 21-28, Elsevier Science 1996.

[4]Nitsche, W., Mirow, P., Szodruch, J., *Piezo-electric foils as a means of sensing unsteady surface forces*, Experiments in Fluids Vol. 7, pp. 111-118, Springer, Germany, 1989.

[5]Peltzer, I., Nitsche, W., *Experimental Investigations of Natural and Controlled Transition on a Laminar Flow Airfoil*, Recent Results in Laminar-Turbulent Transition, Notes on Numerical Fluid Mechanics and Multidisciplinary Design Vol. 86, pp. 269-280, Springer, Germany, 2003.

[6]Domhardt, J., Leuckert, J., Peltzer, I., Nitsche, W., *Measurement of Unsteady Surface Forces by Means of Piezoelectrical Copolymer Coatings*, New Results in Numerical and Experimental Fluid Mechanics VI, Notes on Numerical Fluid Mechanics and Multidisciplinary Design Vol. 96, pp. 96-103, Springer, Germany, 2007.

[7]Engert, M., Pätzold, A., Becker, R., Nitsche, W., *Active Cancellation of TollmienSchlichting Instabilities in Compressible Flows Using Closed-Loop Control*, to be published in IUTAM Symposium on Flow Control and MEMS, Springer, Netherland, 2007.

[8]Hoefener, L., Leuckert, J., Neitzke, K.-P., Hucker, M.J., Warsop, C., Nitsche, W., *Application of Advanced Surface Sensors for the Detection and Control of Flow Separation on an Industrial High-lift Configuration*, ICAS 2006-347, Proceedings of the 25th Congress of the International Council of the Aeronautical Sciences, Germany, 2006.

[9]Sturzebecher, D., Anders, S., Nitsche, W., *The surface hot wire as a means of measuring mean and fluctuating wall shear stress*, Experiments in Fluids Vol. 31, pp. 294-301, Germany, 2001.

[10]Greff, E., *In-flight measurement of static pressures and boundary-layer state with integrated sensors*, Journal of Aircraft Vol. 28, pp. 289299, 1991.

[11]Burkhardt, O., *Erprobung und Anwendung von Oberflächensensoren und Sensorarrays zur Erfassung instationr̈er Wandschubspannungen an Schaufelprofilen*, Ph.D. Thesis, Institute of Aero- and Astronautics, Tech. Univ. Berlin, Mensch und Buch, Germany, 2004.